Differences in temporal adaptation across the human visual hierarchy are explained by delayed divisive normalization

Amber M. Brands (a.m.brands@uva.nl)
Informatics Institute, University of Amsterdam
Science Park 900, 1098 XH, Amsterdam, The Netherlands

Sasha Devore (sasha.devore@nyulangone.org)
New York University School of Medicine
550 First Avenue, NY 10016, New York, USA

Orrin Devinsky (od4@nyu.edu)
New York University School of Medicine
550 First Avenue, NY 10016, New York, USA

Werner Doyle (werner.doyle@nyumc.org)
New York University School of Medicine
550 First Avenue, NY 10016, New York, USA

Adeen Flinker (adeen.flinker@nyulangone.org)
New York University School of Medicine
550 First Avenue, NY 10016, New York, USA

Jonathan Winawer (jonathan.winawer@nyu.edu)
Department of Psychology, New York University
6 Washington Place, NY 10003, New York, USA

Iris I.A. Groen (i.i.a.groen@uva.nl)
Informatics Institute, University of Amsterdam
Science Park 900, 1098 XH, Amsterdam, The Netherlands

This work is licensed under the Creative Commons Attribution 3.0 Unported License.
To view a copy of this license, visit http://creativecommons.org/licenses/by/3.0

Abstract

Neural responses in human visual cortex exhibit adaptation, showing reduced responses to prolonged and to repeated stimuli. While adaptation has been widely observed across the visual cortex, it is unclear to what extent adaptation patterns differ systematically across the visual hierarchy and what neural mechanisms could account for such differences. Here, we identify two signatures of adaptation in time-varying electrocorticography (ECoG) responses that differ between lower and higher visual brain regions. Neural responses in ventral- and lateral-occipitotemporal cortex decay more slowly during sustained stimuli and recover more slowly from adaptation compared to responses in V1-V3. Using a previously proposed model of delayed divisive normalization, we link these differences in adaptation to slower normalization dynamics in higher visual areas. These findings suggest that there are systematic differences in neural adaptation across the visual hierarchy and that history-dependent normalization dynamics offer an explanation for these observed differences.

Keywords: temporal adaptation, delayed divisive normalization, electrocorticography, repetition suppression

Introduction

The human brain integrates sensory inputs over time, evident in transient-decay dynamics for single stimuli and repetition suppression (RS) for repeated stimuli. Adaptation has been widely observed across the visual cortex **(Grill-Spector, Henson, & Martin, 2006)**, but it is debated to what extent adaptation patterns differ across visual brain areas (e.g. **Fritsche, Lawrence, and De Lange (2020)**) and what neural mechanisms may account for it. Recently, a model of delayed divisive normalization (DN), adapted from **Heeger (1992)**, has been shown to predict the level and time course of adaptation in neural responses **(Zhou, Benson, Kay, & Winawer, 2019; Groen et al., 2022)**. The DN model consists of a handful of canonical neural computations and accounts for adaptation in neural response time courses by applying a history-dependent normalization. However, prior studies used simple contrast pattern stimuli which primarily drive responses in low-level areas, making it difficult to compare adaptation patterns across visual cortex. Here, we measured neural responses to naturalistic stimuli at high temporal resolution and spatial precision from human visual cortex to test whether visual areas show area-specific adaptation patterns, and if the DN model can elucidate the underlying neural mechanisms. Neural responses were collected using electrocorticography (ECoG) for single or repeated stimuli belonging to different natural image categories (**Fig. 1**A) with varying temporal conditions. We then characterized differences in adaptation by quantifying transient-decay dynamics and recovery from adaptation in early (V1-V3), ventral-occipitotemporal (VOTC) and lateral-occipitotemporal (LOTC) cortex.

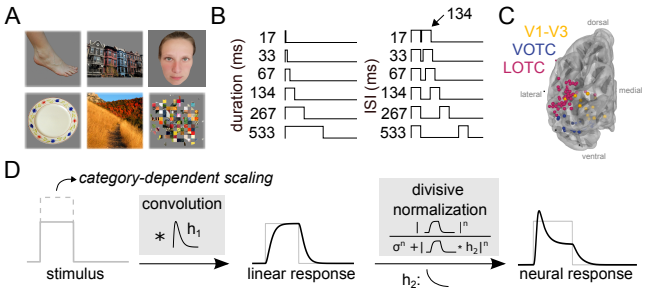

Figure 1: Experimental design. A. Stimulus categories: bodies, houses, faces, objects, scenes and scrambled. B. Time courses of the single (left) and repeated (right) stimuli. C. Electrode positions aggregated across patients. D. Delayed divisive normalization model.

Methods

Experimental procedure

ECoG data was obtained from four epilepsy patients while they viewed naturalistic images, either as single events varying in duration (from 17 to 533 ms), or as two 134-ms events separated by an inter-stimulus interval (ISI) (from 17 to 533 ms) (**Fig. 1**B). Time-varying broadband signals (50-200 Hz) were extracted from a total of 73 visual electrodes with reliable responses. Electrodes were assigned to either V1-V3 (*n = 12*), VOTC (*n = 15*) or LOTC (*n = 46*) (**Fig. 1**C) based on their anatomical location and a probabilistic retinotopic atlas applied to each individual patient **(Wang, Mruczek, Arcaro, & Kastner, 2015)**.

Computational modeling

Per electrode, the broadband time courses were fitted by the DN model (**Fig. 1**D). The core idea is that stimulus-driven activation is divisively normalized by delayed activation history. The normalization is simply the low-pass filtered stimulus-driven activation. First, a linear response, R_L, is computed by convolving a stimulus time course with an impulse response function:

$$R_L = S * h_1(\tau_1), \text{ where } h_1(\tau_1) = te^{-t/\tau_1} \quad (1)$$

where the parameter τ_1 is a time constant determining the time-to-peak of h_1. The input drive is obtained by a full-wave rectification and exponentiation with parameter n of the linear response, $|R_L|^n$. The final step is divisive normalization of this input drive with a low-pass filtered version of R_L (obtained through convolution with an exponential decay function parameterized by τ_2) that is rectified and exponentiated with the same n. In addition, an exponentiated parameter σ is added to the denominator, which prevents the denominator from reaching 0 :

$$R_{DN} = \frac{|R_L|^n}{\sigma^n + |R_L * h_2(\tau_2)|^n}, \text{ where } h_2(\tau_1) = e^{-t/\tau_2} \quad (2)$$

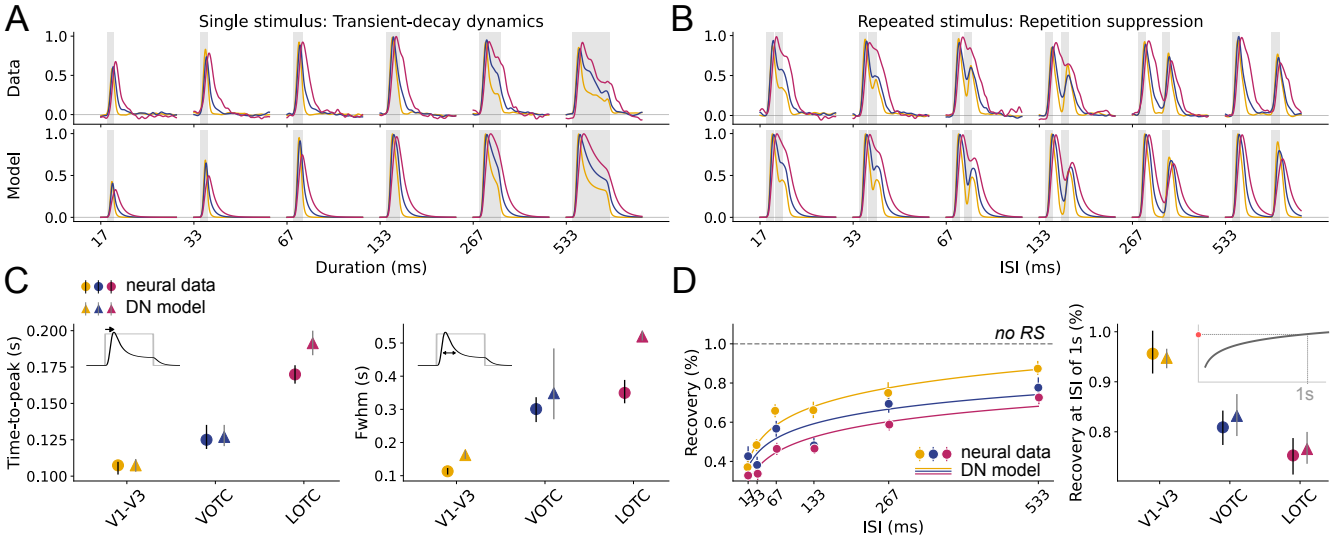

Figure 2: Differences in adaptation patterns in ECoG responses across visual cortex. A. Average broadband (top) and DN model (bottom) bootstrapped (*n = 1000*) time courses for single stimuli with varying durations. B. Same as A but for repeated stimuli with varying ISI. C. Summary metrics derived from neural data (circle) and DN model predictions (triangle) for single stimulus trials. Left: Time to peak. Right: Full-width half-maximum. D. Left: Recovery from adaptation as a function of ISI. Neural data are represented as points and the line is a fitted logged curve, $recovery = a \cdot log(ISI) + c$, where $[a, c]$ are fitted. Right: Degree of recovery for an ISI of 1 s derived from extrapolating the fitted curve for both the neural and model time courses.

To take into account category-selectivity of neural responses in higher visual regions, the DN model scales the input (i.e., the height of the stimulus time course) separately for each stimulus category, adding an additional 6 fitted parameters.

Results

Higher visual areas show slower transient-decay dynamics and slower recovery from adaptation

In all areas, ECoG broadband time courses to single visual stimuli are characterized by transient-decay dynamics, showing higher transients and more prolonged responses for longer duration stimuli (**Fig. 2**A). In addition, all areas exhibit repetition suppression, showing reduced responses to a repeated stimulus for short ISIs and recovery for longer ISIs (**Fig. 2**B). Comparison of these adaptation patterns reveals clear differences between visual areas: across all single stimuli, VOTC and LOTC show a slower response rise (reflected in the time to peak, **Fig. 2**C, left) and more prolonged activation than V1-V3 (reflected in the full-width half max, **Fig. 2**C, right). For repeated stimuli, VOTC and LOTC show stronger repetition suppression compared to V1-V3, with the biggest difference at long ISIs (**Fig. 2**D). Moreover, these area differences are accurately recapitulated by the DN model.

Differences in adaptation reflect slower normalization dynamics in higher visual areas

To explain adaptation differences between areas, we visualized the time courses of two components of the DN model: the input drive (numerator, Eq. 2) and the normalization pool (denominator, Eq. 2) (**Fig. 3**). The DN model captures transient-decay dynamics of single stimuli because the input drive dominates first, resulting in a transient, while the normalization pool dominates later, resulting in a decay. In higher visual areas, both the input drive and the normalization pool rise more slowly, compared to V1-V3 (**Fig. 3**A). The DN model explains RS by predicting activation of the normalization pool that continues to linger after onset of the second stimulus. This normalization activity lingers longer in higher visual areas, leading to slower recovery from adaptation (**Fig. 3**B).

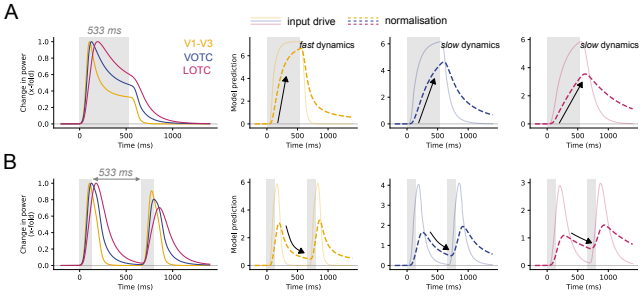

Figure 3: Differences in adaptation patterns reflect normalization pool dynamics. A. Left: Model time courses for a single stimulus for V1-V3, VOTC and LOTC. Right: Input drive (solid) and normalization pool (dashed) activation plotted separately over time. B. Same as A for a repeated stimulus trial.

Conclusion

We reveal differences in adaptation patterns in neural responses across the visual hierarchy and link these to differences in history-dependent divisive normalization.

Acknowledgments

This work was supported by a MacGillavry Fellowship to IIAG and a NIH R01 MH111417 to JW.

References

Fritsche, M., Lawrence, S. J., & De Lange, F. P. (2020). Temporal tuning of repetition suppression across the visual cortex. *Journal of Neurophysiology*, *123*(1), 224–233.

Grill-Spector, K., Henson, R., & Martin, A. (2006). Repetition and the brain: neural models of stimulus-specific effects. *Trends in cognitive sciences*, *10*(1), 14–23.

Groen, I. I., Piantoni, G., Montenegro, S., Flinker, A., Devore, S., Devinsky, O., ... others (2022). Temporal dynamics of neural responses in human visual cortex. *Journal of Neuroscience*, *42*(40), 7562–7580.

Wang, L., Mruczek, R. E., Arcaro, M. J., & Kastner, S. (2015). Probabilistic maps of visual topography in human cortex. *Cerebral cortex*, *25*(10), 3911–3931.

Zhou, J., Benson, N. C., Kay, K., & Winawer, J. (2019). Predicting neuronal dynamics with a delayed gain control model. *PLoS computational biology*, *15*(11), e1007484.